Electronic Supplementary Material (ESI) for Nanoscale.

Supporting Information

Flexible,robust and multifunctional montmorillonite/aramid nanofibers@MXene electromagnetic shielding nanocomposite with an alternating structure for enhanced Joule heating and fire-resistant protective performance

Wanbin Dang[a], Zongxu Liu[a], Lingna Wang[a], Yanhui Chen[*a], Min Qi[*b], Qiuyu Zhang[*a]

[a] *Key Laboratory of Special Functional and Smart Polymer Materials of Ministry of Industry and Information Technology, School of Chemistry and Chemical Engineering, Northwestern Polytechnical University, Xi'an, 710072, P. R. China*

[b] *School of Electronics and Information, Northwestern Polytechnical University, Xi'an, 710072, P. R. China*

**Corresponding Author: Q. Zhang, qyzhang@nwpu.edu.cn; M. Qi, drqimin@nwpu.edu.cn; Y. Chen, yanhuichen@nwpu.edu.cn*

Calculation of electromagnetic interference shielding

The scattering parameters (S11 and S21) were recorded to calculate transmission (T), reflection (R), absorption (A), total EMI SE (SE_T), absorption SE (SE_A) and reflection SE (SE_R) using the following equations:

$$R = |S_{11}|^2 \quad \text{* MERGEFORMAT (1)}$$

$$T = |S_{21}|^2 \quad \text{* MERGEFORMAT (2)}$$

$$SE_R = -10\log(1-R) \quad \text{* MERGEFORMAT (3)}$$

$$SE_A = -10\log\left(T / (1-R) \right) \quad \text{* MERGEFORMAT (4)}$$

$$SE_T = SE_A + SE_R + SE_M \quad \text{* MERGEFORMAT (5)}$$

When $SE_T \geq 10dB$, the SE_M could be negligible. Meanwhile, the EMI shielding efficiency of all samples are converted from the EMI effectiveness (dB) using the following equation:

$$Shielding\ efficiency\ (\%) = 100 - \left(1 / \left(10^{SE/10}\right) \right) \times 100 \text{*}$$

MERGEFORMAT (6)

Table S1 The related parameters of the nanocomposite

Sample	Layer number of MXene	Layer number of AT	each MXene layer	each AT layer
AT2@MX1	1	2	50mg	25mg×2
AT3@MX2	2	3	25mg×2	16.7mg×3
AT4@MX3	3	4	16.7mg×3	12.5mg×4
AT5@MX4	4	5	12.5mg×4	10mg×5

Sample	The content of MXene	The content of ANFs	The content of MMT
MXene	50mg	/	/
AT	/	45mg	5mg
ATM	50mg	45mg	5mg

Figure S1. (a) XRD patterns of Ti_3AlC_2 and d-$Ti_3C_2T_x$, SEM images of Ti_3AlC_2 and TEM images of $Ti_3C_2T_x$ (the corresponding SAED pattern is in the lower inset of panel). (b) XPS spectra of O 1s spectra for d-$Ti_3C_2T_x$.

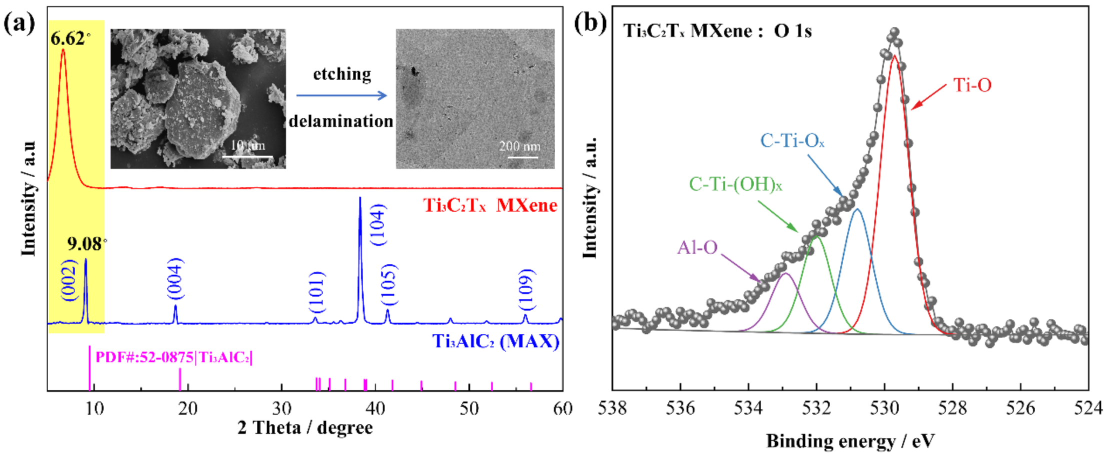

Figure S2. XRD patterns of aramid fiber (AF) and aramid nanofibers (ANFs) , SEM images of AF and TEM images ANFs.

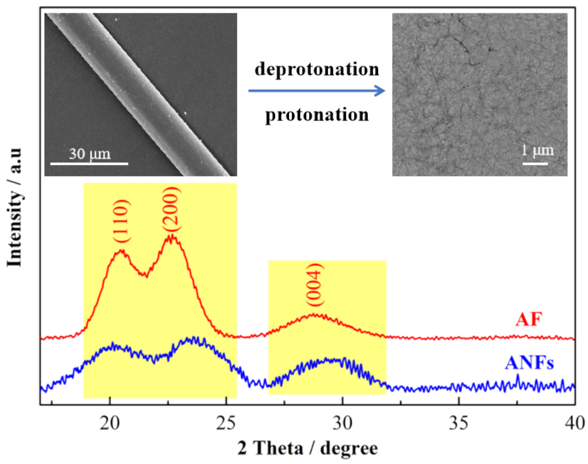

Figure S3. SEM images and EDS mapping images of ATM nanocomposite including surface and cross-sectional.

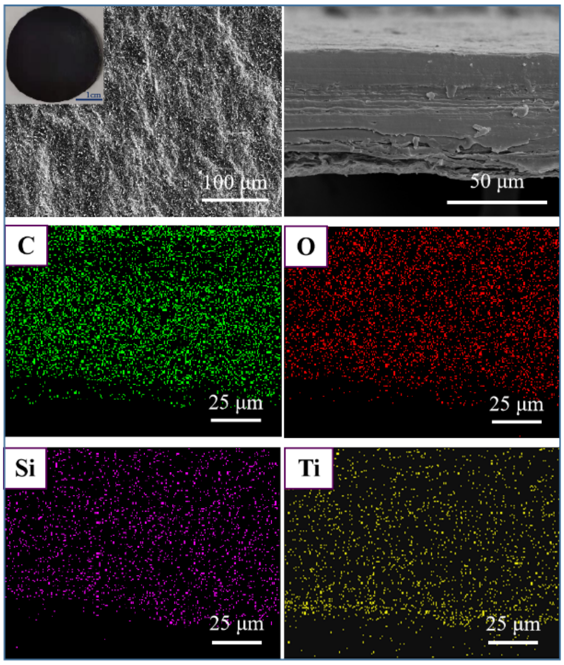

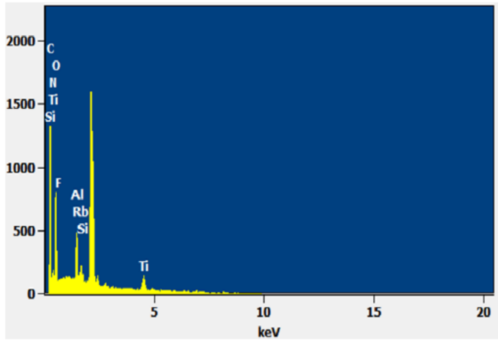

Element	Net Counts	Weight %	Atom %
C K	6751±86	26.57±0.34	41.04±0.52
O K	3501±95	34.87±0.95	40.42±1.10
Ti K	1478±55	26.18±0.97	10.14±0.38
Si K	1027±110	3.92±0.42	2.59±0.28
Al K	2469±111	8.46±0.38	5.82±0.26

Figure S4. The cross-sectional SEM images and the exact weight percentage of all elements in EDS images of AT3@MX2 nanocomposite.

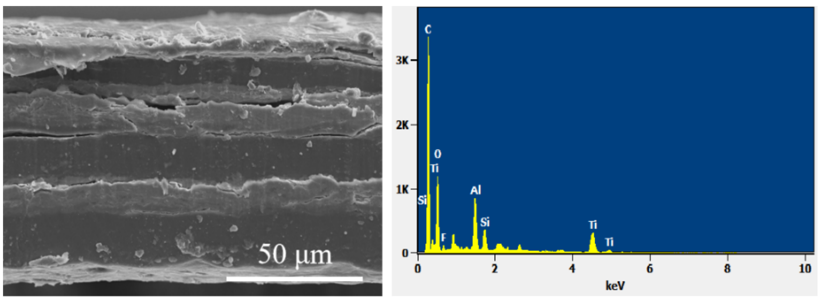

Element	Net Counts	Weight %	Atom %
C K	16567±131	25.86±0.2	41.13±0.33
O K	6781±90	26.97±0.36	32.21±0.43
F K	1704±101	7.02±0.42	7.06±0.42
Ti K	4177±99	28.13±0.66	11.22±0.27
Si K	3011±100	4.4±0.15	2.99±0.1
Al K	5775±108	7.63±0.14	5.4±0.1

Table S2 The EMI shielding efficiency (%) of the nanocomposites

Sample	EMI shielding efficiency (%)
AM	0.619998
MXene	99.999990
ATM	99.994034
AT2@MX1	99.997324
AT3@MX2	99.999712
AT4@MX3	99.999854
AT5@MX4	99.999696

Figure S5 The typical relative resistance change as a function of applied strain curves

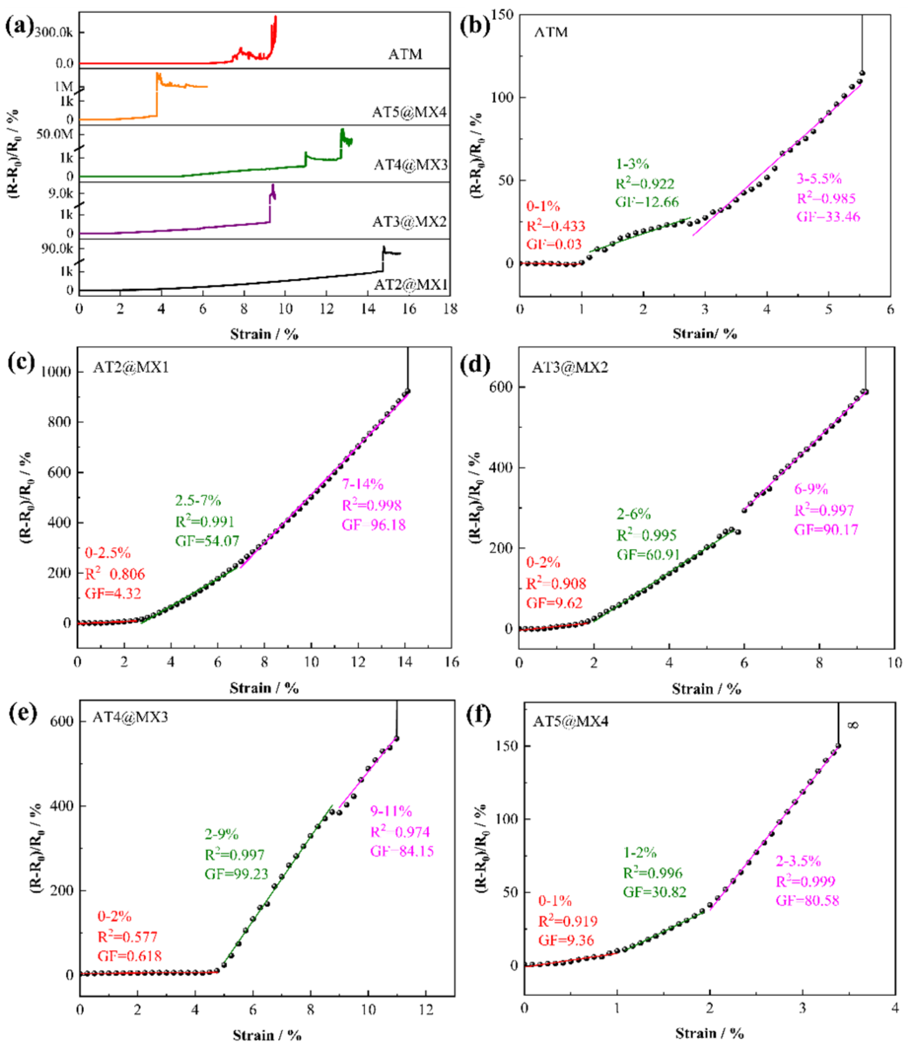

All nanocomposites were tested by an electromechanical universal testing machine (Instron) at room temperature. A Tektronix DMM 4040 6-1/2 digital precision multimeter was connected to record the resistance changes of nanocomposites during the stretch processes, and the gauge factor (GF) was calculated by normalized resistance change ((R-R0)/R0). Figure S5 illustrates the typical relative resistance change as a function of applied strain curves and linear behavior of different nanocomposites' strain.

As depicted in Figure S5, the relative resistance variation $(R-R_0)/R_0$ of all nanocomposites increases with the increasing strain in the whole sensing range, which can be ascribed to the destruction of the conductive layer under stretching. Compared with ATM nanocomposite, the MMT/ANFs@MXene nanocomposites exhibit a high sensibility in a certain strain and performs three linear regimes, especially the AT4@MX3 nanocomposite. The gauge factors (GF) of AT4@MX3 nanocomposite calculated at three different strain ranges: GF=0.618 in the strain range of 0~2%, GF=99.23 in 2~9%, and GF=84.15 in 9 ~11%, which are much higher than that of the traditional metallic strain sensor (GF around 2).

Figure S6. The total EMI SE (SE_T), absorption SE (SE_A) and reflection SE (SE_R) of pure MXene film and AT nanocomposite at the X-band.

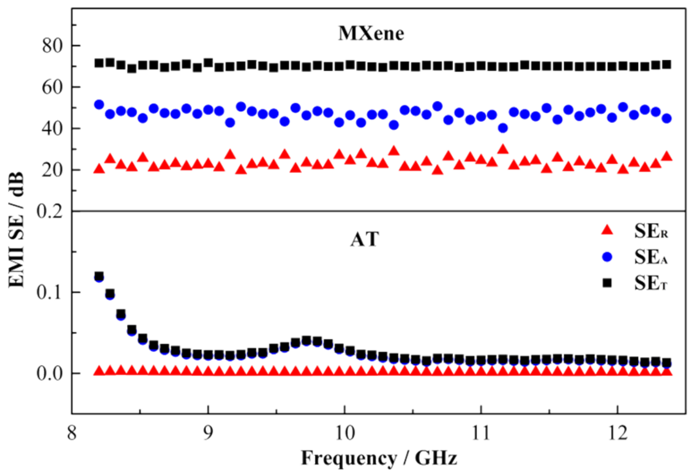

Table S3 The performance comparison of MMT/ANFs@MXene nanocomposites with other materials.

Materials	Filler	Thickness (mm)	SE (dB)	Tensile strength (MPa)	Ref.
d-$Ti_3C_2T_x$/CNFs	d-$Ti_3C_2T_x$	0.167	25.00	135.40	1
HANF/90% EG	expanded graphite	0.030	34.90	24.20	2
CNF5@MXene4	$Ti_3C_2T_x$	0.035	39.60	112.50	3
PU/MX-50	$Ti_3C_2T_x$	0.006	37.90	30.96	4
s-rGO/PS	rGO	2.500	45.10	/	5
GOSN	Ag nanowires	0.018	92.00	/	6
PS/MWCNT	MWCNT	1.800	23.20	/	7
MWCNT/CNF	MWCNT	0.150	46.40	/	8
d-$Ti_3C_2T_x$/ANFs	$Ti_3C_2T_x$	0.017	28.54	80.14	9
cellulose/rGO/Fe_3O_4 aerogel	rGO+Fe_3O_4	0.500	40.10	/	10
CNT-NR	CNT	0.100	30.10	20.60	11
TiO_2-$Ti_3C_2T_x$/graphene	$Ti_3C_2T_x$	0.009	27.00	/	12
$Ti_3C_2T_x$/PEDOT:PSS	$Ti_3C_2T_x$	0.011	42.10	13.71	13
Fe_3O_4@rGO/MWCNT /WPU	MWCNT	0.800	36.00	/	14
Layered ANF-MXene /AgNW	MXene/AgNW	0.056	64.10	148.50	15
Fe_3O_4@$Ti_3C_2T_x$/GF /PDMS	Fe_3O_4@$Ti_3C_2T_x$	1.000	83.60	/	16
GMT/PEFP/GNP	graphite nanoplatelet	2.000	33.80	22.80	17
Au/MWCNT/PVDF	Au/MWCNT	0.500	26.71	/	18

PUDA/CNT	CNT	2.000	35.90	/	19
$NiFe_2O_4$/rGO	/	2.000	38.20	/	20
MXene-Al-II	/	0.005	44.80	83.20	21
MXene/ANF	MXene	0.021	34.60	131.30	22
rGO/CA	rGO	0.012	25.70	118.00	23
RGO/CNF@Ag–Fe_3O_4	Fe_3O_4	0.110	21.00	175.50	24
CNF/RGO	RGO	0.023	26.20	67.70	25
CNFs@PDA@AgNPs	AgNPs	0.111	55.30	17.22	26
CNF/MWCNT/$Ti_3C_2T_x$	$Ti_3C_2T_x$	0.025	51.80	7.60	27
rGO/CNTs/Co/C	/	0.034	51.00	36.17	28
MXene-GO	MXene	0.007	36.89	150.00	29
PTP@MXene	MXene	/	32.00	101.16	30
MXene-xanthan	MXene	0.007	34.10	116.48	31
AM2@MX1	$Ti_3C_2T_x$	0.062	45.73	99.08	This work
AM3@MX2	$Ti_3C_2T_x$	0.076	55.40	154.66	
AM4@MX3	$Ti_3C_2T_x$	0.076	58.38	130.23	
AM5@MX4	$Ti_3C_2T_x$	0.056	55.18	133.50	

References

1. W. T. Cao, F. F. Chen, Y. J. Zhu, Y. G. Zhang, Y. Y. Jiang, M. G. Ma and F. Chen, *ACS Nano*, 2018, **12**, 4583-4593.
2. Y. Liu, K. Zhang, Y. Mo, L. Zhu, B. Yu, F. Chen and Q. Fu, *Compos. Sci. Technol.*, 2018, **168**, 28-37.
3. B. Zhou, Z. Zhang, Y. Li, G. Han, Y. Feng, B. Wang, D. Zhang, J. Ma and C. Liu, *ACS Appl. Mater. Interfaces*, 2020, **12**, 4895-4905.
4. Z. Liu, W. Wang, J. Tan, J. Liu, M. Zhu, B. Zhu and Q. Zhang, *J. Mater. Chem. C*, 2020, **8**, 7170-7180.
5. D. Yan, H. Pang, B. Li, R. Vajtai, L. Xu, P. Ren, J. Wang and Z. Li, *Adv. Funct. Mater.*, 2015, **25**, 559-566.
6. H. J. Sim, D. W. Lee, H. Kim, Y. Jang, G. M. Spinks, S. Gambhir, D. L. Officer, G. G. Wallace and S. J. Kim, *Carbon*, 2019, **155**, 499-505.
7. J. Chen, X. Liao, W. Xiao, J. Yang, Q. Jiang and G. Li, *ACS Sustain. Chem. Eng.*, 2019, **7**, 9904-9915.
8. H. Zhang, X. Sun, Z. Heng, Y. Chen, H. Zou and M. Liang, *Ind. Eng. Chem. Res.*, 2018, **57**, 17152-17160.
9. F. Xie, F. Jia, L. Zhuo, Z. Lu, L. Si, J. Huang, M. Zhang and Q. Ma, *Nanoscale*, 2019, **11**, 23382-23391.
10. Y. Chen, P. Potschke, J. Pionteck, B. Voit and H. Qi, *ACS Appl. Mater. Interfaces*, 2020, **12**, 22088-22098.
11. L. Jia, M. Li, D. Yan, C. Cui, H. Wu and Z. Li, *J. Mater. Chem. C*, 2017, **5**, 8944-8951.
12. C. Xiang, R. Guo, S. Lin, S. Jiang, J. Lan, C. Wang, C. Cui, H. Xiao and Y. Zhang, *Chem. Eng. J.*, 2019, **360**, 1158-1166.
13. R. Liu, M. Miao, Y. Li, J. Zhang, S. Cao and X. Feng, *ACS Appl. Mater. Interfaces*, 2018, **10**, 44787-44795.
14. A. Sheng, W. Ren, Y. Yang, D. Yan, H. Duan, G. Zhao, Y. Liu and Z. Li, *Composites, Part A*, 2020, **129**, 105692.

15. Z. Ma, S. Kang, J. Ma, L. Shao, Y. Zhang, C. Liu, A. Wei, X. Xiang, L. Wei and J. Gu, *ACS Nano*, 2020, **14**, 8368-8382.
16. V. T. Nguyen, B. K. Min, Y. Yi, S. J. Kim and C. G. Choi, *Chem. Eng. J.*, 2020, **393**, 124608.
17. M. Ma, L. Qiao, H. Yu, S. Chen, Y. Shi, H. He and X. Wang, *J. Mater. Sci-Mater. El.*, 2021, **32**, 25863-25875
18. R. Kumaran, S. D. kumar, N. Balasubramanian, M. Alagar, V. Subramanian and K. Dinakaran, *J. Phys. Chem. C*, 2016, **120**, 13771-13778.
19. T. Wang, W. Yu, C. Zhou, W. Sun, Y. Zhang, L. Jia, J. Gao, K. Dai, D. Yan and Z. Li, *Composites, Part B*, 2020, **193**, 108015.
20. A. Kumar, A. K. Singh, M. Tomar, V. Gupta, P. Kumar and K. Singh, *Ceram. Int.*, 2020, **46**, 15473-15481.
21. Z. Liu, Y. Zhang, H. Zhang, Y. Dai, J. Liu, X. Li and Z. Yu, *J. Mater. Chem. C*, 2020, **8**, 1673-1678.
22. C. Lei, Y. Zhang, D. Liu, K. Wu and Q. Fu, *ACS Appl. Mater. Interfaces*, 2020, **12**, 26485-26495.
23. L. Jia, W. Sun, C. Zhou, D. Yan, Q. Zhang and Z. Li, *J. Mater. Chem. C*, 2018, **6**, 9166-9174.
24. T. Guo, C. Li, Y. Wang, Y. Wang, J. Yue and X. Tang, *Appl. Phys. A*, 2020, **126**, 776.
25. W. Yang, Z. Zhao, K. Wu, R. Huang, T. Liu, H. Jiang, F. Chen and Q. Fu, *J. Mater. Chem. C*, 2017, **5**, 3748-3756.
26. Y. Xu, K. Qian, D. Deng, L. Luo, J. Ye, H. Wu, M. Miao and X. Feng, *Carbohydr. Polym.*, 2020, **250**, 116915.
27. K. Qian, H. Wu, J. Fang, Y. Yang, M. Miao, S. Cao, L. Shi and X. Feng, *Carbohydr. Polym.*, 2021, **254**, 117325.
28. M. Yang, Q. Wei, J. Li, Y. Wang, H. Guo, L. Gao, L. Huang, X. He, Y. Li and Y. Yuan, *Adv. Mater. Interfaces*, 2020, **7**, 1901815.
29. J. Liu, Z. Liu, H. Zhang, W. Chen, Z. Zhao, Q. Wang and Z. Yu, *Adv. Electron. Mater.*, 2019, **6**, 1901094.

30. Y. Wang, H. Peng, T. Li, B. Shiu, H. Ren, X. Zhang, C. Lou and J. Lin, *Chem. Eng. J.*, 2021, **412**, 128681.
31. Y. Sun, R. Ding, S. Hong, J. Lee, Y.-K. Seo, J.-D. Nam and J. Suhr, *Chem. Eng. J.*, 2021, **410**, 128348.